JACS
JOURNAL OF THE AMERICAN CHEMICAL SOCIETY
Article
pubs.acs.org/JACS

Developing Quinoidal Fluorophores with Unusually Strong Red/Near-Infrared Emission

Longbin Ren,[†,‡] Feng Liu,[†,‡] Xingxing Shen,[†,‡] Cheng Zhang,[†,‡] Yuanping Yi,*[,†] and Xiaozhang Zhu*[,†]

[†]Beijing National Laboratory for Molecular Sciences, CAS Key Laboratory of Organic Solids, Institute of Chemistry, Chinese Academy of Sciences, Beijing 100190, P. R. China

[‡]University of Chinese Academy of Sciences, Beijing 100049, P. R. China

Supporting Information

ABSTRACT: Despite the dominant position of aromatic fluorophores, we report herein the design and synthesis of quinoidal fluorophores based on rarely emissive quinoidal bithiophene. Quinoidal bitheno[3,4-*b*]thiophene, **QBTT-C6**, consisting of cruciform-fused (*E*)-1,2-bis(5-hexylthiophen-2-yl)ethene and quinoidal bithiophene, shows a fluorescence quantum yield of 8.5%, 25-fold higher than that of the parent quinoidal **QBT** chromophore, but its maximum emission is at similar wavelengths. **QBTT-Ar**'s featuring intramolecular charge transfer can further shift the maximum emission into the near-infrared region. The intramolecular charge transfer is programmably enhanced by tuning the substituents on the aryl groups from the electron-withdrawing trifluoromethyl to the electron-donating methoxy groups. Unexpectedly, a positive relationship between intramolecular charge transfer and fluorescence quantum yield is observed; as a result, **QBTT-FL** gives an unprecedentedly high fluorescence quantum yield of up to 53.1% for quinoidal oligothiophenes. With detailed photophysical and theoretical investigations, we demonstrate that the nonradiative intersystem crossing ($S_1 \rightarrow T_2$) is significantly restrained in **QBTT-Ar**'s, which can be attributed to the faster reverse intersystem crossing ($T_2 \rightarrow S_1$) characteristic of a small activation energy. This work reveals the possibility for developing red/near-infrared fluorophores from the less explored quinoidal molecules because of their intrinsically narrow bandgaps.

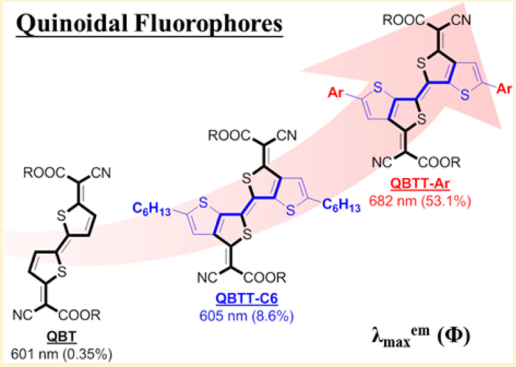

INTRODUCTION

Fluorescence,[1] an important feature affiliated with π-conjugated molecular systems, has been widely utilized for sensing, imaging, labeling, display, and illumination. Recently, near-infrared (NIR) fluorescence[2] has received special interest because of its ability to penetrate deeply into tissues without interference from autofluorescence[3] and its electroluminescence application in NIR organic light-emitting diodes (OLEDs).[4] Compared with massive organic dyes with UV–vis emission, NIR fluorophores possessing high fluorescence quantum yields (Φ) are relatively few, which can be explained by the energy gap law:[5] the luminescence efficiency of organic molecules reduces with decreasing energy gap. As shown in Figure 1, borondipyrromethenes (BODIPYs),[6] cyanines,[7] and squaraines[8] are the classical fluorescent scaffolds for the design of NIR fluorophores by judicious molecular modifications. It is generally held that "most fluorescent compounds are aromatic."[1] Quinoidal conjugated molecules with Kekulé structures, such as quinoidal oligothiophenes,[9] porphyrins,[10] and hydrocarbons,[11] can seldom be utilized for fluorescence applications because of their negligible emissions. However, quinoidal molecules usually have intrinsically narrow bandgaps, high transition probability of S_0 (the ground state) → S_1 (the first singlet state),[12] and should function as potentially excellent NIR fluorophores once the deleterious nonemissive channel can be unraveled and effectively blocked.

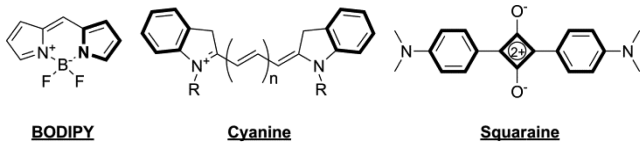

Figure 1. Classical NIR fluorescent scaffolds (The aromatic parts are highlighted with bold lines).

Quinoidal oligothiophenes (**QOTs**)[9] are important organic optoelectronic materials because of their unique properties such as high electron affinity, narrow optical bandgap,[13] biradical property,[14] and excellent electron-transporting ability.[15] The fluorescence of **QOTs** is extremely weak and has rarely been mentioned in past research.[16] Casado et al.[17] proposed that the nonradiative process of quinoidal terthiophene (**QTT**) may originate from the $S_1 \rightarrow T_2$ (the second triplet excited state) intersystem crossing (ISC) because of the small energy difference between the S_1 and T_2 states. In the previous work on oligo-*p*-quinodimethanes (***p*-OQMs**),[18] we found that the internal conversion (IC) could not account for the weak

Received: April 15, 2015
Published: August 20, 2015

DOI: 10.1021/jacs.5b03899
J. Am. Chem. Soc. 2015, 137, 11294–11302

fluorescence property considering the molecular rigidity of the *p*-**OQM**s. Thus, we assume that the fluorescence channel of **QOT**s could possibly be switched on by restraining the nonradiative ISC process via proper modulation of the relative S_1 and T_2 energy levels.

We report herein the design and synthesis of quinoidal fluorescent motifs, **QBTT**s, that can be viewed as cruciform-fused molecules consisting of aromatic (*E*)-1,2-bis(5-arylthiophen-2-yl)ethene (**BTE-Ar**'s) and quinoidal bithiophene (**QBT**) subunits by sharing five alternating single−double carbon−carbon bonds (Scheme 1). **QBTT-C6** with hexyl

Scheme 1. Quinoidal Fluorophores, QBTT-Ar's

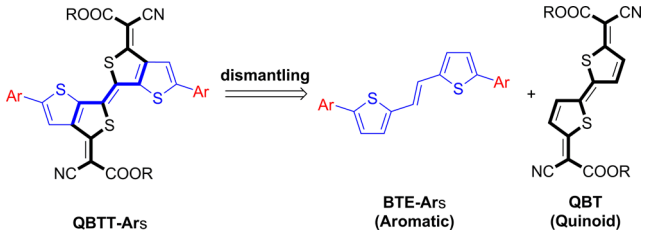

groups shows a fluorescence quantum yield of 8.5%, 25-fold higher than that of the parent quinoidal **QBT** chromophore, but with the maximum emission at a similar wavelength. By introducing aryl groups to the **QBTT** scaffold, we found that **QBTT-Ar**'s are even stronger fluorescent emitters and approach the NIR region. When the electron-donating ability of the substituents on the aryl groups is systematically elevated, both the luminescent efficiency and intramolecular charge transfer (ICT) are enhanced, which apparently violates the general understanding. Compared with the parent **QBT** (Φ: 0.35% in toluene), the fluorescence quantum yields of **QBTT-Ar**'s are significantly increased by up to 2 orders of magnitude. Through detailed photophysical studies, we attribute this high fluorescence enhancement of **QBTT-Ar**'s to the restriction of the ISC nonradiative process between S_1 and T_2 states, which can arise from the small and relatively lower activation energies for the reverse ISC (RISC) relative to the ISC processes, as supported by theoretical investigations.

RESULTS

Synthesis of QBTT-Ar's. Synthesis of the **QBTT** core was tricky because of the difficult manipulation of the highly electron-rich thieno[3,4-*b*]thiophene (**TT**) unit. After numerous attempts, we finally found that a route from trimethyl(thieno[3,4-*b*]thiophen-2-yl)silane (**TT-TMS**, **1**)[19] is suitable for its synthesis, as shown in Scheme 2a. 2-Chlorothieno[3,4-*b*]thiophene (**TT-Cl**, **2**) was obtained from **TT-TMS** by chlorination at the 2-position of the **TT** anion formed in situ at room temperature (rt) in 58% yield. Bromination of **TT-Cl** proceeded efficiently with *N*-bromosuccinimide (NBS) to give 4,6-dibromo-2-chlorothieno[3,4-*b*]thiophene **3** in 78% yield as a white solid. The structure of bench-stable **3** was confirmed by single-crystal X-ray analysis. (4-Bromo-2-chlorothieno[3,4-*b*]-thiophen-6-yl)lithium can be formed by selective Li−Br exchange[15] between **TT-BrCl** and *n*-BuLi. The key multifunctionalized 4,4′-dibromo-2,2′-dichloro-6,6′-bithieno[3,4-*b*]-thiophene (**BTT-BrCl**, **4**) was successfully obtained in 70% yield as a brown solid from oxidative homocoupling of (4-bromo-2-chlorothieno[3,4-*b*]thiophen-6-yl)lithium with copper(II) chloride. With **BTT-BrCl** in hand, the key functionalized building block, **QBTT-Cl**, was synthesized by Pd-catalyzed selective coupling of **TT-BrCl** and (1-cyano-2-(octyloxy)-2-oxoethyl)sodium followed by air oxidation[20] as a dark-green solid in 30% yield. Finally, **QBTT-Ar**'s were obtained in good yields of 55−72% by Suzuki-type cross-coupling[21] between **QBTT-Cl** and various arylboronic aids with substituents bearing different electronic properties. As an alkyl-substituted reference, **QBTT-C6**, with two hexyl groups was also synthesized, but with a different synthetic route, as shown in Scheme 2b. The head-to-head dimer **8** was synthesized in 31% yield as an orange solid by Stille-type cross-coupling between 2-hexyl-6-iodothieno[3,4-*b*]thiophene

Scheme 2. Synthesis of QBTT-Ar's (a), and the Reference QBTT-C6 (b)[a]

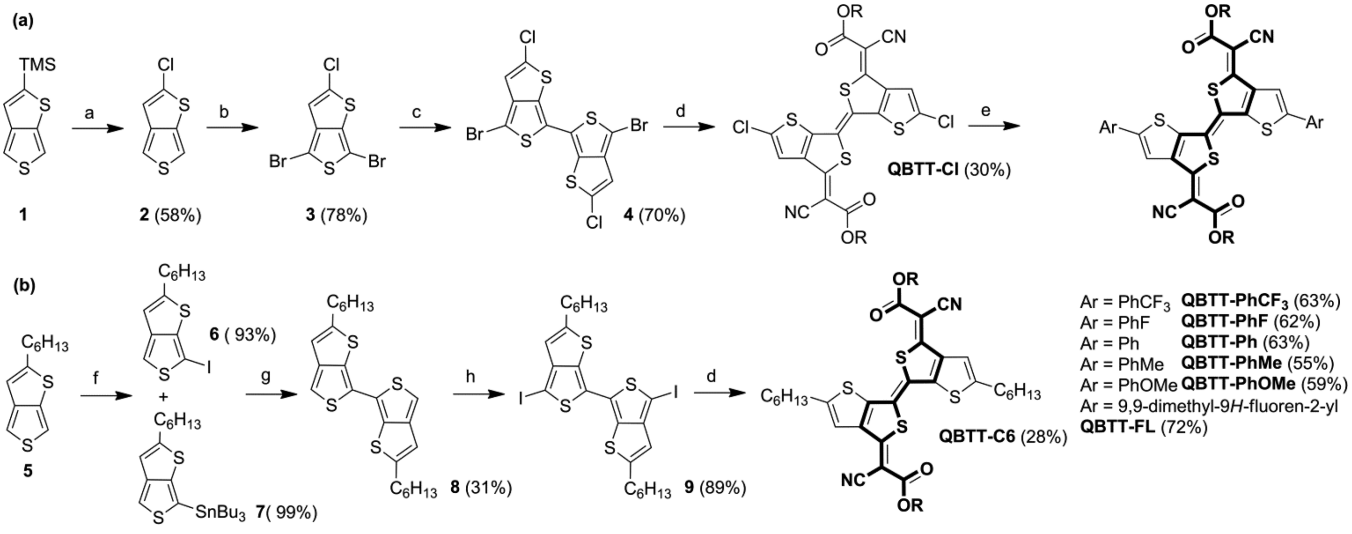

[a]Reagents and conditions: (a) *n*-Bu_4NF, hexachloroethane, diethyl ether, rt; (b) NBS, $CHCl_3$, rt; (c) (i) *n*-BuLi, Et_2O, −40 °C; (ii) $CuCl_2$; (d) (i) octyl 2-cyanoacetate, NaH, $Pd(PPh_3)_4$, 1,4-dioxane, 100 °C; (ii) HCl, air, rt; (e) $Pd(P^tBu_3)_2$, arylboronic acid, CsOH, THF/H_2O (4:1); (f) (i) *n*-BuLi, THF, −78 °C; (ii) diiodoethane (for **6**), tributylchlorostannane (for **7**); (g) $Pd(PPh_3)_4$, toluene/DMF, 100 °C; (h) (i) *n*-BuLi, THF, −78 °C; (ii) diiodoethane.

DOI: 10.1021/jacs.5b03899
J. Am. Chem. Soc. 2015, 137, 11294−11302

(**6**) and tributyl(2-hexylthieno[3,4-*b*]thiophen-6-yl)stannane (**7**), the syntheses of which were reported in our previous work.[15a] 2,2′-Dihexyl-4,4′-diiodo-6,6′-bithieno[3,4-*b*]thiophene **9** was synthesized in 89% yield by deprotonation of compound **8** at the 4,4′-positions with *n*-BuLi followed by iodination with diiodoethane. With a similar Pd-catalyzed coupling reaction, **QBTT-C6** was obtained smoothly in 28% yield. All the compounds were unambiguously confirmed by NMR and high-resolution mass spectra or elemental analysis.

QBTT-Cl, **QBTT-Ar**'s, and **QBTT-C6** have a high C_{2h} symmetry with stable *E*-configuration, which results in relatively simple NMR spectra that do not evolve with time. For example, **QBTT-Cl** showed a single peak (δ 8.01 ppm) in the aromatic region that can be assigned to the β-hydrogens of the fused thiophenes with magnetic equivalence. The detailed structure of **QBTT-Cl** is unambiguously confirmed by single-crystal X-ray analysis. As shown in Figure 2, **QBTT-Cl** exhibits a planar molecular structure. Differing from **QBT** that undergoes *E*/*Z* isomerization,[15,22] **QBTT-C6** shows a stable *E*-configuration, which may be related to the multiple weak intramolecular interactions because the distances of 2.736 Å for O−S and 3.233 Å for S−S are shorter than the sum of O, S (3.32 Å) and S, S (3.60 Å) van der Waals radii.[23] Besides, DFT calculations at the B3LYP/6-31G** level show that the energy of the optimized *Z* form is 3.94 kcal/mol higher than that of the optimized *E* form in **QBTT-Cl**, which may also contribute to the stable *E*-configuration.

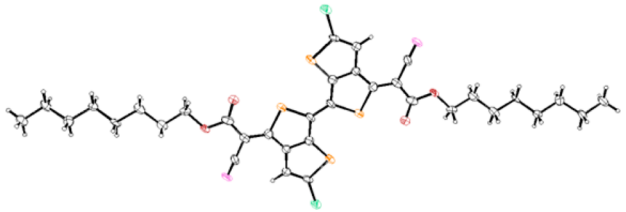

Figure 2. Molecular structures of **QBTT-Cl** with 50% probability ellipsoids.

Photophysical Properties of QBT, BTE, and QBTT's. Compound **QBTT-C6** with two hexyl groups can be viewed as a molecular combination of aromatic (*E*)-1,2-bis(5-hexylthiophen-2-yl)ethene (**BTE-C6**) and quinoidal **QBT**. The absorption spectra of the three compounds in dilute toluene solution are shown in Figure 3a and relevant data are summarized in Table 1. **BTE-C6** shows typical short-wavelength absorption in the UV region with an absorption coefficient (ε) of 3.50 × 10^4 L^{-1} M^{-1} and large S_1 energy of 3.16 eV. In agreement with the quinoidal molecular structure, **QBT** shows intensive and long-wavelength absorption with a high ε of 8.42 × 10^4 L^{-1} M^{-1} and small S_1 energy of 2.14 eV. The hybrid **QBTT-C6** exhibits structured absorption with an ε of 9.66 × 10^4 L^{-1} M^{-1} and S_1 energy of 2.09 eV, which are similar to those of **QBT**; this indicates that the incorporation of **BTE-C6** makes the molecular configuration of the S_1 state of **QBTT-C6** relatively more rigid but only slightly decreases the S_1 energy. This is fully consistent with our theoretical results (Table S1). The calculated excitation energy for the S_1 state is decreased by only ca. 0.08 eV from **QBT** to **QBTT-Me**. The fluorescence spectra of **QBT** and **QBTT-C6** are similar (Figure S1), with maximum emission at around 600 nm. Interestingly, compared with the very weak emissive nature of **QBT** (Φ: 0.35%), **QBTT-C6** exhibits a fluorescence quantum yield of 8.6%, which is 25-fold higher.

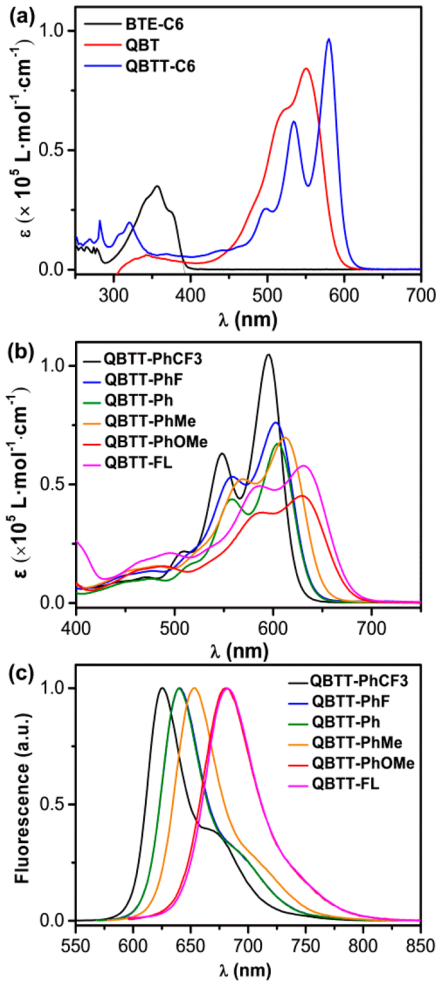

Figure 3. UV−vis-NIR absorption spectra of **QBTT-C6**, **QBT**, and **BTE-C6** (a), **QBTT-Ar**'s (b), and fluorescence spectra of **QBTT-Ar**'s (c) in toluene.

Because the introduction of ICT can effectively reduce optical bandgaps by hybridization of the energy levels of the donor and acceptor, **QBTT-Ar**'s with different aryl groups were synthesized with programmable S_1 energy levels deriving from the enhanced electron-donating ability of the aromatic **BTE-Ar**'s. As seen from Figure 4 and Table S2, the S_1 state exhibits an obvious charge transfer from the phenyl groups to the **QBT** backbone. Thus, the maximum absorption of **QBTT-Ph** (λ_{max}^{abs}, 605 nm; S_1 energy, 1.99 eV) is bathochromically shifted by 25 nm relative to that of **QBTT-C6** (λ_{max}^{abs}, 580 nm; S_1 energy, 2.09 eV). A similar red-shift (35 nm) for the maximum emission is observed from **QBTT-C6** (605 nm) to **QBTT-Ph** (640 nm). Most strikingly, contrary to the popular belief that increasing ICT will lead to a decrease of luminescence efficiency, the Φ of **QBTT-Ph** (36.6%) is 4-fold higher than that of **QBTT-C6** (8.6%).

The optical properties of **QBTT-Ar**'s can be further tuned by modification of the substituents on the aryl groups. As seen from Figure 3, the absorption and emission spectra of **QBTT-Ph** are blue/red-shifted by electron-withdrawing/donating substitutions. Compared with **QBTT-PhCF3**, the emission peak of **QBTT-PhOMe** exhibits a bathochromic shift as large as 55 nm, extending to 680 nm (approaching the NIR region).

DOI: 10.1021/jacs.5b03899
J. Am. Chem. Soc. 2015, 137, 11294−11302

Table 1. Photophysical and Electrochemical Properties of BTE-C6, QBT, QBTT-C6, and QBTT-Ar's[a]

compound	λ_{max}^{abs} (nm)	ε ($\times 10^4$ L^{-1} M^{-1})	λ_{max}^{em} (nm)[e]	Φ (%)[b]	τ_F (ns)[d]	k_r ($\times 10^8$ s^{-1})[e]	k_{nr} ($\times 10^8$ s^{-1})[e]	E_{LUMO} (eV)[c,f]	E_{HOMO} (eV)[g]	S_1[h] (eV)[g]
QBT	550	8.42	601	0.35	0.016	2.19	634.72	−4.04	−6.14	2.14
BTE-C6	356	3.50	416	5.1 (3.5)[c]	0.19	2.68	49.96	–[j]	–[j]	3.23
QBTT-C6	580	9.66	605	8.6 (4.1)[c]	0.55	1.56	16.62	−3.82	−5.88	2.09
QBTT-PhCF3	596	10.5	625	21.2 (5.0)[c]	2.32	0.91	3.40	−3.93	−5.92	2.03
QBTT-PhF	602	7.61	640	26.2 (9.4)[c]	2.90	0.90	2.54	−3.89	−5.85	2.00
QBTT-Ph	605	6.70	640	36.6 (14.1)[c]	2.82	1.30	2.25	−3.88	−5.84	1.99
QBTT-PhMe	612	6.96	652	32.5 (18.2)[c]	3.40	0.96	1.96	−3.87	−5.76	1.96
QBTT-PhOMe	628	4.52	680	42.4 (22.6)[c]	4.36	0.97	1.32	−3.86	−5.70	1.90
QBTT-FL	630	5.78	682	53.1	4.38	1.21	1.07	−3.88	−5.71	1.89

[a]Measured in toluene. [b]Fluorescence quantum yield was determined by the absolute method. [c]Measured in dichloromethane. [d]Fluorescence lifetime. [e]The rates of radiative and nonradiative processes were determined by $k_r = \Phi/\tau_F$ and $k_{nr} = (1 - \Phi)/\tau_F$. [f]The LUMO energy levels were determined by $E_{LUMO} = -(4.80 + E_{red}^{1/2})$ (eV). [g]$E_{HOMO} = E_{LUMO} - E_g^{opt}$, $E_g^{opt} = 1240/\lambda_{onset}$ (eV). [h]Determined from the average energy of the absorption and emission maxima. [j]Not examined.

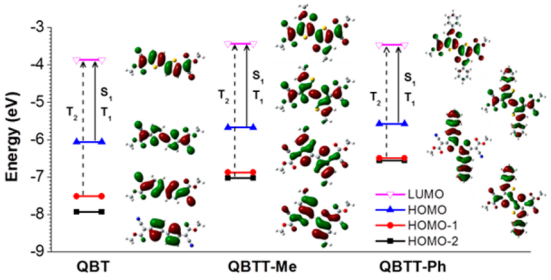

Figure 4. Illustration of molecular orbitals and energy levels as well as main transitions for S_1, T_1, and T_2 calculated by TD-DFT at the B3LYP/6-31G** level in the gas phase based on the ground-state geometries for **QBT**, **QBTT-Me**, and **QBTT-Ph**.

However, the fluorescence quantum yield is systematically enhanced from 21.2% to 42.4% by increasing the electron-donating strength of the aryl group, as shown in Table 1; this contradicts the general understanding that ICT is harmful to Φ because of the reduction of the transition dipole. The gradually enhanced ICT from **QBTT-PhCF3**, **QBTT-Ph** to **QBTT-PhOMe** can be qualitatively distinguished by Lippart-Mataga solvent dependence analysis. By performing linear correlation between Stokes shift and Lippart-Mataga solvent polarizability,[24] we found that the Stokes shift of **QBTT-PhOMe** is most sensitive to the solvent polarizability among the three compounds (Figure S2). It should be noted that the ICT nature of the S_1 state for the **QBTT-Ar**'s compounds is further confirmed by the decreased Φ in a solvent (CH_2Cl_2) with higher polarity (Table 1). When we extend the π-system with rigid 2-fluorenyl substituents, **QBTT-FL** gives the longest emission wavelength of 682 nm at the peak and the highest Φ of 53.1% in this series, which is 6-fold higher than that of **QBTT-C6** and may be due to its strongest ICT effect as revealed in Figure S2.

Electrochemical Properties of QBT and QBTT's. All quinoidal compounds exhibit two typical reversible reduction processes (Figure S11). Compared with the parent **QBT**, the first reduction potential of **QBTT-C6** is negatively shifted by 0.22 V, which can be attributed to the stabilization of the quinoidal structure by fusing aromatic thiophene units. Attaching further aryl groups to **QBTT** only slightly affects the lowest occupied molecular orbital (LUMO) energy levels. As determined from the half-wave reduction potentials, the LUMO energy levels for **QBTT-PhCF3** and **QBTT-PhOMe** are −3.93 and −3.86 eV, respectively. As indicated by theoretical calculations, the LUMO orbitals of **QBTT-Ar**'s are mainly localized on the **QBTT** subunit (Figure 4). However, the highest occupied molecular orbital (HOMO) energy levels, as estimated from the optical bandgaps and LUMO energy levels, are more sensitive to electronic properties of the substituents, e.g., −5.92 eV for **QBTT-CF3** vs −5.70 V for **QBTT-OMe**, because the HOMOs of **QBTT-Ar**'s are delocalized to the aryl groups.[14a]

DISCUSSION

To understand the intriguing fluorescence enhancement from **QBT** and **QBTT-C6** to **QBTT-Ph**, we have examined the excited-state dynamic processes. Generally, Φ is determined by the radiative and nonradiative rates of the S_1 state. In dilute solutions, the nonradiative processes are constituted by IC and ISCs. Because of reductions in emission energies and oscillator

Table 2. Adiabatic Excitation Energies of S_1, T_1, and T_2 States; Reorganization Energies (λ) and Activation Energies (E_a) for Transitions between S_1 and T_2; and Reorganization Energies and Oscillator Strengths for Transition from S_1 to S_0[a]

				$S_1 \rightarrow T_2$		$T_2 \rightarrow S_1$		$S_1 \rightarrow S_0$	
compound	S_1	T_1	T_2	λ	E_a	λ	E_a	λ	f
QBT	2.287	0.750	2.104	0.129	0.006	0.118	0.192	0.106	1.093
QBTT-Me	2.208	0.957	2.168	0.143	0.018	0.103	0.050	0.099	0.925
QBTT-Ph	1.956	0.917	1.988	0.052	0.034	0.057	0.003	0.127	0.768
QBTT-PhCF3	2.013	0.935	2.041	0.078	0.036	0.074	0.007	0.128	0.891
QBTT-PhMe	1.895	0.904	1.926	0.038	0.031	0.046	0.001	0.123	0.752
QBTT-PhOMe	1.774	0.877	1.785	0.021	0.012	0.021	0.001	0.114	0.686

[a]Calculated by the time-dependent density functional theory (TD-DFT) at the B3LYP/6-31G** level in the gas phase (all energies in eV).

DOI: 10.1021/jacs.5b03899
J. Am. Chem. Soc. 2015, 137, 11294−11302

strengths, the measured radiative rate of S_1 is decreased from **QBT** (2.19×10^8 s^{-1}), to **QBTT-C6** (1.56×10^8 s^{-1}), to **QBTT-Ph** (1.30×10^8 s^{-1}) (Tables 1 and 2). On the other hand, both the decrease in emission energy and the enhancement in reorganization energy (0.099 eV for **QBTT-C6** and 0.127 eV for **QBTT-Ph**, Table 2), as revealed by calculations, suggest that the IC rate would be increased for **QBTT-Ph**. However, experimental measurements show that the nonradiative rate is substantially decreased in the order **QBT** (6.35×10^{10} s^{-1}), **QBTT-C6** (1.66×10^9 s^{-1}), and **QBTT-Ph** (2.25×10^8 s^{-1}). Thus, ISC should be responsible for the more significant nonradiative decay of S_1 and the lower Φ in **QBTT-C6** and especially in **QBT**. As Table 2 and Table S1 show, while the excitation energy of T_1 is much lower than that of S_1 for these compounds, the energies of S_1 and T_2 are quite close, with the energy difference within 0.2 eV. For **QBTT-Ph**, the T_2 state lies above the S_1 state. However, the T_2 energy levels of **QBT** (2.104 eV) and **QBTT-C6** (2.168 eV) are smaller relative to S_1, especially for **QBT** (2.287 eV). Along with the reorganization energy, the activation energy for ISC from $\mathbf{S_1}$ to $\mathbf{T_2}$ is estimated to be 6, 18, and 34 meV for **QBT**, **QBTT-C6**, and **QBTT-Ph**, respectively (see Supporting Information for more computational details). This indicates that the ISC from S_1 to T_2 can be thermally activated for these compounds. In particular, the ISC process can be even ultrafast for **QBT**. More interestingly, the activation energy for RISC from T_2 to S_1 is very large for **QBT**, reaching 192 meV; the RISC process is hence completely forbidden (Figure 5a),

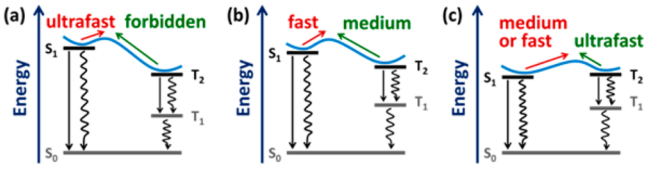

Figure 5. Schematic illustration of excited-state dynamics in (a) **QBT**, (b) **QBTT-C6**, and (c) **QBTT-Ph** derivatives.

leading to quenching of fluorescence. However, the corresponding activation energy from T_2 to S_1 is much smaller for **QBTT-C6** (50 meV) and becomes extremely small for **QBTT-Ph** (3 meV). Therefore, S_1 can be partially recovered from T_2 through RISC for **QBTT-C6** (Figure 5b). For **QBTT-Ph**, the RISC process should not be a bottleneck (Figure 5c), leading to the great enhancement in Φ. The experimental observation that the fluorescence intensity of **QBTT-Ph** is increased 2-fold when the temperature is decreased from 80 °C to room temperature is in agreement with our deduction that the main nonradiative decay should be ascribed to thermally activable ISC.

Similarly to **QBTT-Ph**, the theoretical calculations indicate that although T_2 is thermally accessible from S_1, the RISC process will be much faster for all the substituted compounds. This is consistent with the relatively higher Φ with respect to **QBTT-C6**. Interestingly, T_2 and T_3 are energetically degenerate for **QBTT-PhCF3** (Table S1 and Figure S12), so there is an additional ISC nonradiative channel to reduce Φ. As the electron-donating strength of the aryl group is increased, the energy gap between T_3 and T_2 is increased (Table S1); then the possibility of ISC involving T_3 will be smaller, leading to an enhanced Φ. Finally, it should be noted that the competition between the radiative and nonradiative decay processes of T_2 to T_1 and of S_1 to S_0 can play an important role in the accurate determination of the Φ values among all the molecular systems, which will require further exhaustive photophysical investigation.

CONCLUSION

We have successfully developed new fluorophores, **QBTT-Ar**'s, based on the rarely emissive quinoidal bithiophenes. **QBTT-C6** consisting of cruciform-fused (*E*)-1,2-bis(5-hexylthiophen-2-yl)ethene and quinoidal bithiophenes shows enhanced fluorescence with a fluorescence quantum yield of 8.5%, 25-fold higher than that of the parent quinoidal **QBT** chromophore with maximum emission at similar wavelengths. Introduction of ICT by attaching aryl groups to **QBTT** can further shift the maximum emissions into the NIR region. The ICT can be programmably enhanced by tuning the substituents on the aryl groups, from the electron-withdrawing trifluoromethyl to the electron-donating methoxy groups. Positively related ICT and fluorescence quantum yield is unexpectedly observed, which gives high quantum yields of up to 53.1% (682 nm, **QBTT-FL**), unprecedented in quinoidal oligothiophenes. With detailed photophysical and theoretical investigations, we find that the nonradiative ISC ($S_1 \rightarrow T_2$), the overwhelming deactivation process in **QBT**, is significantly restrained in **QBTT-Ar**'s, which we ascribe to the fast reverse ISC ($T_2 \rightarrow S_1$) because of the reduced activation energy. Considering the reverse ISC in the high triplet excited state, we believe that **QBTT-Ar**'s will be excellent electroluminescence candidates for OLED applications,[4a,25] which may exceed the spin-statistics limit,[26] a crucial issue for obtaining highly efficient fluorescent OLEDs.[27] Our work also reveals the possibility for developing near-infrared fluorophores from the less explored quinoidal molecules with intrinsically narrow bandgaps, which may emerge as a new family of fluorophores corresponding to the aromatic counterparts.

EXPERIMENTAL SECTION

Materials and General Methods. All the reactions dealing with air- or moisture-sensitive compounds were carried out in a dry reaction vessel under a positive pressure of nitrogen. Unless stated otherwise, starting materials were obtained from Adamas, Aldrich, and J&K and were used without any further purification. Anhydrous THF, toluene, and 1,4-dioxane were distilled over Na/benzophenone prior to use. Anhydrous DMF was distilled over CaH_2 prior to use. Trimethyl(thieno[3,4-*b*]thiophen-2-yl)silane (**1**),[19] 2-hexylthieno[3,4-*b*]-thiophene (**5**),[28] and tributyl(2-hexylthieno[3,4-*b*]thiophen-4-yl)-stannane (**7**)[15] were prepared according to the published procedures. Hydrogen nuclear magnetic resonance (^{1}H NMR) and carbon nuclear magnetic resonance (^{13}C NMR) spectra were measured on Bruker Fourier 300, Bruker Avance 400, and Bruker Avance 600 spectrometers. Chemical shifts for hydrogens are reported in parts per million (ppm, δ scale) downfield from tetramethylsilane and are referenced to the residual protons in the NMR solvent ($CDCl_3$: δ 7.26). ^{13}C NMR spectra were recorded at 100 MHz. Chemical shifts for carbons are reported in parts per million (ppm, δ scale) downfield from tetramethylsilane and are referenced to the carbon resonance of the solvent ($CDCl_3$: δ 77.2). The data are presented as follows: chemical shift, multiplicity (s = singlet, d = doublet, t = triplet, m = multiplet and/or multiple resonances, br = broad), coupling constant in hertz (Hz), and integration. EI−MS measurements were performed on UK GCT-Micromass or Shimadzu G-MS-QP2010 spectrometers. MALDI measurements were performed on MALDI-FT 9.4T, Bruker solariX, or MALDI-TOF MS Bruker Autoflex III. Elemental analyses were measured on Flash EA 1112 Series from ThermoQuest. UV−vis and fluorescence spectra were recorded on a Jasco V-570 and Jasco FP-6600 spectrometers, respectively. Cyclic voltammetry (CV) was

DOI: 10.1021/jacs.5b03899
J. Am. Chem. Soc. 2015, 137, 11294−11302

performed on a CHI620D potentiostat. All measurements were carried out in a one-compartment cell under an N_2 atmosphere, equipped with a glassy-carbon electrode, a platinum counter-electrode, and an Ag/Ag^+ reference electrode with a scan rate of 100 mV/s. The supporting electrolyte was a 0.1 mol/L dichloromethane solution of tetrabutylammonium perchlorate (TBAP). All potentials were corrected against Fc/Fc^+. CV was measured with a scan rate of 100 mV/s. Thermogravimetric analysis (TGA) was performed on a Shimadzu DTG 60 instrument at a heating rate of 10 °C min^{-1} under an N_2 atmosphere with runs recorded from room temperature to 550 °C. Fluorescent quantum yields (FLQY) were measured on Absolute PL Quantum Yield Spectrometer C11347 from Hamamatsu. Individual microplates were investigated at room temperature in air using a homemade optical microscope equipped with a 50 × 0.9 NA excitation objective. The second harmonic (400 nm, 150 fs, 1 kHz) of a regenerative amplifier (Spitfire, Spectra Physics) seeded with a mode-locked Ti:sapphire laser (Tsunami, Spectra Physics) was focused to a 50-μm-diameter spot to excite the selected individual microplate. Then, PL spectra were collected underneath by using a 100× 0.9 NA objective that was mounted on a 3D movable stage. A 420 nm long-wave pass dielectric filter was used to block any scattered excitation light. Finally, the collected PL was coupled to an optical fiber with diameter 25/125 μm (core/cladding) and detected using a liquid-nitrogen-cooled CCD (SPEC-10-400B/LbN, Roper Scientific) attached to a polychromator (Spectropro-550i, Acton). The spectral resolution was 0.1 nm. Time-resolved PL was detected with a streak camera (C5680, Hamamatsu Photonics) dispersed by a polychromator (250is, Chromex) with a spectral resolution of 1 nm and a time resolution of 10 ps.

2-Chlorothieno[3,4-*b*]thiophene (2). Perchloroethane (2.471 g, 10.44 mmol) was added to an oven-dried Schlenk tube containing compound **1** (2.016 g, 9.50 mmol) in dry THF (40 mL) under an argon atmosphere. After a stirring period of 10 min, tetrabutylammonium fluoride (TBAF) (10 mL, 10 mmol, 1.0 mol/L in dry THF) was added slowly via a dry syringe. After a stirring period of another hour, the reaction mixture was quenched with a few drops of saturated NH_4Cl solution and extracted with diethyl ether three times. The organic layer was combined, dried over $MgSO_4$, and concentrated under reduced pressure. The crude product was purified using silica-gel column chromatography (hexane) to give 0.89 g of compound **2** in 58% yield as a light-yellow oil. ^{1}HNMR (400 MHz, $CDCl_3$): δ 6.871 (s, 1H), 7.18 (d, ^4J = 2.4 Hz, 1H), 7.27 (d, ^4J = 2.4 Hz, 1H). ^{13}C NMR (100 MHz, $CDCl_3$): δ 111.1, 111.9, 116.3, 136.385, 136.428, 143.9. HRMS (EI) calcd for $C_6H_3ClS_2$ $[M]^+$: 173.9365, found 173.9367.

4,6-Dibromo-2-chlorothieno[3,4-*b*]thiophene (3). NBS was added in batches at 0 °C in the dark to a round-bottomed flask containing compound **2** (2.676 g, 15.32 mmol) dissolved in $CHCl_3$ (50 mL). After a stirring period of 2 h, the reaction mixture was quenched with a few drops of saturated NH_4Cl solution; extracted with CH_2Cl_2 three times,; and washed with saturated $NaHSO_3$ solution, saturated $NaHCO_3$ solution, and saturated NaCl solution. The organic layer was combined, dried over $MgSO_4$, and concentrated under reduced pressure. The crude product was purified by recrystallization and gave 3.984 g of compound **3** in 78% yield as a white needle-like solid. ^{1}H NMR (400 MHz, $CDCl_3$): δ 6.76 (s, 1H). ^{13}C NMR (100 MHz, $CDCl_3$): δ 96.9, 97.4, 116.6, 137.4, 138.2, 143.7. Anal. Calcd for C_6HBr_2Cl (%): C, 21.68; H, 0.3. Found: C, 21.77; H, <0.3. HRMS (EI) calcd for $C_6HBr_2ClS_2$ $[M]^+$: 331.7554, found 331.7558.

4,4′-Dibromo-2,2′-dichloro-6,6′-bithieno[3,4-*b*]thiophene (4). An oven-dried Schlenk tube containing compound **3** (1.0 g, 3.0 mmol) in dry Et_2O (120 mL) under an argon atmosphere was cooled to −40 °C and *n*-butyllithium (1.9 mL, 3.1 mmol, 1.60 M in hexane) was then added slowly via a syringe. After a stirring period of about an hour, $CuCl_2$ (0.89 g, 6.6 mmol) was added to the reaction mixture. After about an hour, the temperature was slowly raised to room temperature overnight. Then, the reaction mixture was quenched with a few drops of saturated NH_4Cl solution and filtered to isolate the brown crude product, which was washed three times with ammonium hydroxide to give 0.587 g of compound **4** in 70% yield as a dark-brown solid. ^{1}HNMR (300 MHz, $CDCl_3$): δ 6.82 (s, 2H). HRMS (MALDI-TOF) calcd for $C_{12}H_2Br_2Cl_2S_4$ $[M]^+$: 501.677765, found 501.678169.

2-Hexyl-6-iodothieno[3,4-*b*]thiophene (6). Compound **5** (0.22 g, 1.0 mmol) was dissolved in anhydrous THF (4 mL) under a nitrogen atmosphere and cooled to −78 °C, and *n*-butyllithium (0.66 mL, 1.05 mmol, 1.60 M in hexane) was then added via a syringe under stirring. After a stirring step at −78 °C for 0.5 h, 1,2-diiodoethane (0.31 g, 1.10 mmol) was added in one portion and the mixture stirred at −78 °C for another 0.5 h. Then, the clear reaction solution was warmed to room temperature over 0.5 h. The reaction mixture was quenched with a few drops of saturated NH_4Cl solution, washed with saturated $NaHSO_3$ solution and saturated $NaHCO_3$ solution, and extracted three times with CH_2Cl_2. The organic layer was separated, dried over $MgSO_4$, and concentrated under reduced pressure. A total of 0.32 g of compound **6** was obtained as a light-yellow oil in 93% yield and was used for the next step without further purification. ^{1}H NMR (400 MHz, $CDCl_3$): δ 0.87−0.91 (t, 3H), 1.26−1.40 (m, 6H), 1.68 (m, 2H), 2.75 (t, ^3J = 7.2 Hz, 2H), 6.71 (s, 1H), 7.19 (s, 1H). ^{13}C NMR (100 MHz, $CDCl_3$): δ 14.1, 22.5, 28.7, 30.2, 31.5, 32.1, 56.5, 114.4, 116.5, 146.8, 147.0, 153.5. HRMS (EI) calcd for $C_{12}H_{15}IS_2$ $[M]^+$: 349.9660, found 349.9663.

2,2′-Dihexyl-6,6′-bithieno[3,4-*b*]thiophene (8). Compound **7** (0.552 g, 1.07 mmol) and $Pd(PPh_3)_4$ (53 mg, 0.039 mmol) were added to an oven-dried round-bottomed flask containing compound **6** (0.32 g, 0.93 mmol) in dry DMF (3 mL) and toluene (3 mL) under a nitrogen atmosphere. The mixture was stirred and refluxed for 36 h in the dark. The reaction mixture was then cooled to room temperature and added to 50 mL of MeOH to precipitate the product. The crude product was purified using silica-gel column chromatography (hexane). Further recrystallization gave 0.133 g of compound **8** in 31% yield as a brown solid. ^{1}HNMR (400 MHz, $CDCl_3$): δ 0.88−0.91 (t, 6H), 1.32−1.43 (m, 12H), 1.70−1.77 (m, 4H), 2.79−2.83 (t, 4H), 6.63 (s, 2H), 7.17 (s, 2H). ^{13}C NMR (100 MHz, $CDCl_3$): δ 14.1, 22.6, 28.8, 30.3, 31.6, 32.0, 109.2, 113.7, 122.2, 133.9, 147.8, 153.8. HRMS (MALDI-TOF) calcd for $C_{24}H_{30}S_4$ $[M]^-$: 446.122486, found 446.122690.

2,2′-Dihexyl-4,4′-diiodo-6,6′-bithieno[3,4-*b*]thiophene (9). Compound **8** (0.055 g, 0.12 mmol) was dissolved in anhydrous Et_2O (5 mL) under a nitrogen atmosphere and cooled to 0 °C, and *n*-butyllithium (1.50 mL, 2.40 mmol, 1.60 M in hexane) was then added via a syringe. After a stirring step at 0 °C for 0.5 h, 1,2-diiodoethane (0.16 g, 0.26 mmol) was added in one portion and the mixture was stirred at 0 °C for another 0.5 h before the clear reaction solution was warmed to room temperature over 0.5 h. The reaction mixture was quenched with a few drops of saturated NH_4Cl solution, washed with saturated $NaHSO_3$ solution and saturated $NaHCO_3$ solution, and extracted with CH_2Cl_2 three times. The organic layer was combined, dried over $MgSO_4$, and concentrated under reduced pressure. A total of 0.087 g of compound **9** was obtained as a yellow solid in 89% yield and was used for the next step directly without further purification. ^{1}H NMR (400 MHz, $CDCl_3$): δ 0.87−0.90 (t, 6H), 1.26−1.56 (m, 12H), 1.73 (m, J = 7.2 Hz, 4H), 2.80 (t, ^3J = 7.2 Hz, 4H), 6.46 (s, 1H). ^{13}C NMR (100 MHz, $CDCl_3$): δ 14.1, 22.5, 28.8, 30.3, 31.5, 32.1, 114.8, 127.2, 132.9, 152.9, 155.3. HRMS (MALDI-TOF) calcd for $C_{24}H_{28}I_2S_4$ $[M]^+$: 697.915782, found 697.916015.

(2*Z*,2′*Z*)-Dioctyl 2,2′-((*E*)-2,2′-dichloro-4*H*,4′*H*-[6,6′-bithieno-[3,4-*b*]thiophenylidene]-4,4′-diylidene)bis(2-cyanoacetate) (QBTT-Cl). Sodium hydride (0.64 g, 16.0 mmol) was added to a suspension of octyl 2-cyanoacetate (1.578 g, 8.0 mmol) in anhydrous dioxane (80 mL) under a nitrogen atmosphere and the mixture was stirred for 20 m at room temperature. Compound **4** (0.404 g, 0.8 mmol) and $Pd(PPh_3)_4$ (139 mg, 0.12 mmol) were added to this mixture, which was then heated under reflux. After 8 h, the mixture was cooled to room temperature, and then diluted hydrochloric acid (1.0 M, 10 mL) was added slowly and stirred under an oxygen atmosphere at room temperature for 30 min. The resulting mixture was extracted with CH_2Cl_2 (3 × 50 mL), washed with brine, and dried over $MgSO_4$. After evaporation of the solvent, the residue was purified using silica-gel column chromatography with CH_2Cl_2 followed by washing with hexane and CH_2Cl_2 twice to give 0.274 g of **QBTT-Cl** in

DOI: 10.1021/jacs.5b03899
J. Am. Chem. Soc. 2015, 137, 11294−11302

30% yield as a dark-green solid. ^{1}H NMR (400 MHz, $CDCl_3$): δ 0.89 (t, 6H), 1.26−1.44 (br, 20H), 1.79 (m, ^3J = 7.2 Hz, 4H), 4.37 (t, 4H), 8.01 (s, 2H). ^{13}C NMR (75 MHz, $CDCl_3$): δ 14.1, 22.6, 25.8, 28.6, 29.17, 29.20, 31.8, 67.4, 90.4, 115.1, 122.0, 128.1, 141.8, 142.6, 144.1, 158.0, 164.1. HRMS (MALDI-TOF) calcd for $C_{34}H_{36}Cl_2N_2O_4S_4$ $[M]^-$: 734.094046, found 734.092985.

(2*Z*,2′*Z*)-Bis(2-hexyldecyl)-2,2′-((*E*)-2,2′-dichloro-4*H*,4′*H*-[6,6′-bithieno[3,4-*b*]thiophenylidene]-4,4′-diylidene)bis(2-cyanoacetate) (HD-QBTT-Cl). Dark-green solid in 30% yield. ^{1}H NMR (400 MHz, $CDCl_3$): δ 0.87 (t, 12H), 1.29−1.39 (br, 48H), 1.80 (m, ^3J = 6 Hz, 2H), 4.28 (d, 4H), 8.01 (s, 2H). ^{13}C NMR (100 MHz, $CDCl_3$): δ 14.13, 22.67, 22.70, 26.66, 26.70, 29.3, 29.57, 29.60, 30.0, 31.1, 31.8, 31.9, 37.3, 53.4, 70.0, 90.4, 115.1, 122.1, 128.2, 141.7, 142.7, 144.2, 158.1, 164.3. HRMS (MALDI-TOF) calcd for $C_{50}H_{68}Cl_2N_2O_4S_4$ $[M]^-$: 958.344447, found 958.344578.

(2*Z*,2′*Z*)-Bis(2-decyltetradecyl)-2,2′-((*E*)-2,2′-dichloro-4H,4′H-[6,6′-bithieno[3,4-*b*]thiophenylidene]-4,4′-diylidene)-bis(2-cyanoacetate) (DT-QBTT-Cl). Dark-green solid in 29% yield. ^{1}H NMR (300 MHz, $CDCl_3$): δ 0.87 (t, 12H), 1.25−1.37 (br, 80H), 1.80 (m, ^3J = 6.3 Hz, 2H), 4.28 (d, 4H), 8.01 (s, 2H). ^{13}C NMR (100 MHz, $CDCl_3$): δ 14.1, 22.7, 26.7, 29.4, 29.6, 29.69, 29.71, 29.73, 29.9, 31.1, 31.9, 37.3, 70.0, 90.4, 115.1, 122.1, 128.2, 141.7, 142.7, 144.2, 158.1, 164.3. HRMS (MALDI-TOF) calcd for $C_{66}H_{100}Cl_2N_2O_4S_4$ $[M]^-$: 1182.594848, found 1182.593770.

(2*Z*,2′*Z*)-Dioctyl 2,2′-((*E*)-2,2′-dihexyl-4*H*,4′*H*-[6,6′-bithieno-[3,4-*b*]thiophenylidene]-4,4′-diylidene)bis(2-cyanoacetate) (QBTT-C6). Sodium hydride (0.027 g, 0.68 mmol) was added to a suspension of octyl 2-cyanoacetate (0.067 g, 0.34 mmol) in anhydrous dioxane (1.0 mL) under a nitrogen atmosphere and the mixture was stirred for 20 min at room temperature. Compound **9** (0.024 g, 0.034 mmol) and $Pd(PPh_3)_4$ (6.0 mg, 0.005 mmol) were added to this mixture, which was then heated under reflux. After 8 h, the reaction was cooled to room temperature, diluted hydrochloric acid (1.0 M, 10 mL) was added slowly, and the mixture was stirred under an oxygen atmosphere at room temperature for 30 min. The resulting mixture was extracted with CH_2Cl_2 (3 × 10 mL), washed with brine, and dried over $MgSO_4$. After evaporation of the solvent, the residue was purified using silica-gel column chromatography with CH_2Cl_2 followed by washing with hexane and CH_2Cl_2 twice to give 7.8 mg of **QBTT-C6** in 28% yield as a yellow-green solid. ^{1}H NMR (300 MHz, $CDCl_3$): δ 0.87−0.91 (t, 12H), 1.29−1.43 (br, 32H), 1.77 (m, 8H), 2.92 (t, 4H), 4.36 (t, 4H), 7.76 (s, 2H). ^{13}C NMR (100 MHz, $CDCl_3$): δ 14.0, 14.1, 22.5, 22.7, 25.8, 28.6, 28.8, 29.2, 31.5, 31.7, 31.8, 66.9, 76.7,77.0, 77.3, 88.6, 116.1, 119.7, 128.0, 144.9, 146.1, 158.9, 159.7, 164.8. HRMS (MALDI-TOF) calcd for $C_{46}H_{62}N_2O_4S_4$ $[M]^-$: 834.359791, found 834.359619.

General Procedure for QBTT-PhR (R = CF_3, F, H, Me, OMe) and QBTT-FL. $Pd(OAc)_2$ (30 mmol %) and dicyclohexyl(2′,4′,6′-triisopropyl-[1,1′-biphenyl]-2-yl)phosphine (XPhos) (36 mmol %) was added to a Schlenk tube containing compound **QBTT-Cl** (1 equiv) and *p*-arylboronic acid (4 equiv) in THF (2 mL) and H_2O (0.5 mL) under a nitrogen atmosphere. CsOH aqueous solution (50 wt %, 3.4 equiv) was added to the reaction mixture and heated overnight at 40 °C. The reaction mixture was then cooled to room temperature and extracted with CH_2Cl_2, washed with brine, and dried over $MgSO_4$. Purification using silica-gel column chromatography (hexane/CH_2Cl_2) gave deep-blue or black solids.

(2*Z*,2′*Z*)-Dioctyl 2,2′-((*E*)-2,2′-diphenyl-4*H*,4′*H*-[6,6′-bithieno[3,4-*b*]thiophenylidene]-4,4′-diylidene)bis(2-cyanoacetate) (QBTT-Ph). Yield: 63%. ^{1}H NMR (400 MHz, $CDCl_3$): δ 0.88−0.90 (t, 6H), 1.30−1.44 (br, 20H), 1.77−1.80 (m, ^3J = 7.2 Hz, 4H), 4.28−4.30 (t, ^3J = 7.2 Hz, 4H), 7.43−7.44 (d, ^3J = 6.4 Hz 6H), 7.68−7.70 (d, ^3J = 6.0 Hz, 4H), 8.19 (s, 2H). ^{13}C NMR (100 MHz, $CDCl_3$): δ 14.1, 22.7, 25.8, 28.5, 29.2, 29.3, 31.8, 66.9, 89.2, 115.7, 117.5, 126.1, 128.1, 129.2, 129.7, 132.3, 145.4, 155.8, 158.9, 164.3. HRMS (MALDI-TOF) calcd for $C_{46}H_{46}N_2O_4S_4$ $[M]^-$: 818.235533, found 818.234185.

(2*Z*,2′*Z*)-Dioctyl 2,2′-((*E*)-2,2′-di-*p*-tolyl-4*H*,4′*H*-[6,6′-bithieno[3,4-*b*]thiophenylidene]-4,4′-diylidene)bis(2-cyanoacetate) (QBTT-PhMe). Yield: 55%. ^{1}H NMR (400 MHz, $CDCl_3$): δ 0.89−0.90 (t, 6H), 1.25−1.43 (br, 20H), 1.77−1.83 (m, ^3J = 6.8 Hz, 4H), 2.41 (s, 6H), 4.30−4.33 (t, ^3J = 7.2 Hz, 4H), 7.21−7.23 (d, ^3J = 8.0 Hz 4H), 7.55−7.57 (d, ^3J = 8.0 Hz, 4H), 8.11 (s, 2H). ^{13}C NMR (100 MHz, $CDCl_3$): δ 14.1, 21.4, 22.7, 25.8, 28.6, 29.3, 29.3, 31.8, 66.8, 88.9, 115.7, 116.5, 125.8, 127.8, 128.8, 129.5, 129.8, 130.9, 140.0, 144.8, 145.3, 155.9, 158.8, 164.2. HRMS (MALDI-TOF) calcd for $C_{48}H_{50}N_2O_4S_4$ $[M]^-$: 846.265891; found, 846.264745.

(2*Z*,2′*Z*)-Dioctyl 2,2′-((*E*)-2,2′-bis(4-methoxyphenyl)-4*H*,4′*H*-[6,6′-bithieno[3,4-*b*]thiophenylidene]-4,4′-diylidene)bis(2-cyanoacetate) (QBTT-PhOMe). Yield: 59%. ^{1}H NMR (400 MHz, $CDCl_3$): δ 0.91 (t, 6H), 1.26−1.43 (br, 20H), 1.76−1.78 (m, ^3J = 6.8 Hz, 4H), 3.87 (s, 6H), 4.27 (t, 4H), 6.89−6.91 (d, ^3J = 8.0 Hz 4H), 7.54−7.56 (d, ^3J = 8.0 Hz, 4H), 7.99 (s, 2H). ^{13}C NMR (100 MHz, $CDCl_3$): δ 14.1, 22.7, 25.8, 28.5, 29.3, 29.4, 31.9, 55.3, 66.8, 88.6, 114.3, 115.5, 124.8, 127.2, 127.5, 144.1, 145.1, 155.6, 15.8, 160.7, 164.0. HRMS (MALDI-TOF) calcd for $C_{48}H_{50}N_2O_6S_4$ $[M]^-$: 878.255720, found 878.255888.

(2*Z*,2′*Z*)-Bis(2-hexyldecyl)-2,2′-((*E*)-2,2′-bis(4-(trifluoromethyl)phenyl)-4*H*,4′*H*-[6,6′-bithieno[3,4-*b*]-thiophenylidene]-4,4′-diylidene)bis(2-cyanoacetate) (QBTT-PhCF3). Yield: 63%. ^{1}H NMR (400 MHz, $CDCl_3$): δ 0.85−0.89 (t, 12H), 1.27−1.43 (br, 48H), 1.82 (m, 2H), 4.3 (d, 4H), 7.69, 7.71 (d, ^3J = 8.4 Hz, 4H), 7.79, 7.81 (d, ^3J = 8.4 Hz, 4H), 8.29 (s, 2H). ^{13}C NMR (100 MHz, $CDCl_3$): δ 164.45, 158.63, 153.69, 146.22, 145.53, 135.61, 128.43, 126.41, 126.35, 124.59, 122.79, 119.08, 115.45, 90.15, 70.01, 37.35, 31.93, 31.83, 31.12, 30.01, 29.65, 29.61, 29.37, 26.72, 26.68, 22.70, 14.12. HRMS (MALDI-TOF) calcd for $C_{64}H_{76}F_6N_2O_4S_4$ $[M]^-$: 1178.459761, found 1178.460108.

(2*Z*,2′*Z*)-Bis(2-decyltetradecyl)-2,2′-((*E*)-2,2′-bis(4-fluoro phenyl)-4*H*,4′*H*-[6,6′-bithieno[3,4-*b*]thiophenylidene]-4,4′-diylidene)bis(2-cyanoacetate) (QBTT-PhF). Yield: 62%. ^{1}H NMR (300 MHz, $CDCl_3$): δ 0.84−0.88 (t, 12H), 1.25−1.39 (br, 80H), 1.83 (m, 2H), 4.30 (d, 4H), 7.17 (t, ^3J = 8.4 Hz, 4H), 7.69−7.74 (m, 4H), 8.20 (s, 2H). ^{13}C NMR (100 MHz, $CDCl_3$): δ 14.1, 22.7, 26.7, 26.9, 29.4, 29.65, 29.69, 29.73, 30.01, 30.09, 31.0, 31.1, 32.0, 37.3, 40.6, 65.8, 69.8, 89.5, 115.6, 116.4, 116.6, 117.6, 128.16, 128.24, 128.7, 128.8, 145.5, 145.6, 154.6, 158.9, 162.4, 164.5, 164.9. HRMS (MALDI-TOF) calcd for $C_{78}H_{108}F_2N_2O_4S_4$ $[M]^-$: 1302.716549, found 1302.714899.

(2*Z*,2′*Z*)-Bis(2-hexyldecyl)-2,2′-((*E*)-2,2′-bis(9,9-dimethyl-9*H*-fluoren-2-yl)-4*H*,4′*H*-[6,6′-bithieno[3,4-*b*]thiophenylidene]-4,4′-diylidene)bis(2-cyanoacetate) (QBTT-FL). Yield: 72%. ^{1}H NMR (300 MHz, $CDCl_3$): δ 0.85−0.89 (t, 12H), 1.26−1.43 (br, 48H), 1.59 (s, 12H),1.82 (m, 2H), 4.3 (d, 4H), 7.37−7.40 (m, 2H), 7.45−7.49 (m, 1H), 7.70−7.86 (t, 4H), 8.32 (s, 2H). ^{13}C NMR (100 MHz, $CDCl_3$): δ 14.1, 22.69, 22.71, 26.69, 26.72, 27.1, 29.4, 29.59, 29.65, 30.0, 31.2, 31.8, 31.9, 37.3, 47.3, 69.7, 89.3, 115.9, 117.7, 120.5, 120.8, 122.7, 125.8, 127.2, 128.1, 128.3, 131.6, 138.1, 141.2, 145.5, 145.8, 154.2, 154.8, 156.7, 159.4, 164.9. HRMS (MALDI-TOF) calcd for $C_{80}H_{94}N_2O_4S_4$ $[M]^-$: 1274.610192, found 1274.609904.

■ ASSOCIATED CONTENT

Supporting Information

The Supporting Information is available free of charge on the ACS Publications website at DOI: 10.1021/jacs.5b03899.

Cyclic voltammograms, Lippart-Mataga solvent-dependence analyses, NMR spectra, theoretical calculation details (PDF)

Crystallographic file of compound **QBTT-Cl** (CIF)

Crystallographic file of compound **3** (CIF)

■ AUTHOR INFORMATION

Corresponding Authors

*xzzhu@iccas.ac.cn

*ypyi@iccas.ac.cn

Notes

The authors declare no competing financial interest.

DOI: 10.1021/jacs.5b03899
J. Am. Chem. Soc. 2015, 137, 11294−11302

■ ACKNOWLEDGMENTS

We thank the National Basic Research Program of China (973 Program) (No. 2014CB643502, 2014CB643506), the Strategic Priority Research Program of the Chinese Academy of Sciences (XDB12010200, XDB12020200), and the National Natural Science Foundation of China (91333113) for financial support. We thank Prof. Yishi Wu for his help on fluorescence lifetime measurements.

■ REFERENCES

(1) Valeur, B.; Berberan-Santos, M. N. *Molecular Fluorescence: Principles and Applications*, 2nd ed.; Wiley-VCH: Weinheim, Germany, 2013.

(2) (a) Holtrup, F. O.; Müller, G. R. J.; Quante, H.; Feyter, S. D.; Schryver, F. C. D.; Müllen, K. *Chem.—Eur. J.* **1997**, *3*, 219. (b) Geerts, Y.; Quante, H.; Platz, H.; Mahrt, R.; Hopmeier, M.; Böhm, A.; Müllen, K. *J. Mater. Chem.* **1998**, *8*, 2357. (c) Qian, G.; Wang, Z. Y. *Chem. - Asian J.* **2010**, *5*, 1006.

(3) (a) Guo, Z.; Park, S.; Yoon, J.; Shin, I. *Chem. Soc. Rev.* **2014**, *43*, 16. (b) Yuan, L.; Lin, W.; Zheng, K.; He, L.; Huang, W. *Chem. Soc. Rev.* **2013**, *42*, 622. (c) Achilefu, S. *Angew. Chem., Int. Ed.* **2010**, *49*, 9816. (d) Escobedo, J. O.; Rusin, O.; Lim, S.; Strongin, R. M. *Curr. Opin. Chem. Biol.* **2010**, *14*, 64. (e) Hilderbrand, S. A.; Weissleder, R. *Curr. Opin. Chem. Biol.* **2010**, *14*, 71. (f) Kiyose, K.; Kojima, H.; Nagano, T. *Chem. - Asian J.* **2008**, *3*, 506.

(4) (a) Yao, L.; Zhang, S.; Wang, R.; Li, W.; Shen, F.; Yang, B.; Ma, Y. *Angew. Chem., Int. Ed.* **2014**, *53*, 2119. (b) Qian, G.; Zhong, Z.; Luo, M.; Yu, D.; Zhang, Z.; Wang, Z. Y.; Ma, D. *Adv. Mater.* **2009**, *21*, 111. (c) Nepomnyashchii; Bard, A. J. *Acc. Chem. Res.* **2012**, *45*, 1844.

(5) Englman, R.; Jortner, J. *Mol. Phys.* **1970**, *18*, 145.

(6) (a) Lu, H.; Mack, J.; Yang, Y.; Shen, Z. *Chem. Soc. Rev.* **2014**, *43*, 4778. (b) Boens, N.; Leen, V.; Dehaen, W. *Chem. Soc. Rev.* **2012**, *41*, 1130. (c) Frath, D.; Massue, J.; Ulrich, G.; Ziessel, R. *Angew. Chem., Int. Ed.* **2014**, *53*, 2290. (d) Loudet, A.; Burgess, K. *Chem. Rev.* **2007**, *107*, 4891.

(7) (a) Doja, M. Q. *Chem. Rev.* **1932**, *11*, 273. (b) Mishra, A.; Behera, R. K.; Behera, P. K.; Mishra, B. K.; Behera, G. B. *Chem. Rev.* **2000**, *100*, 1973. (c) Fischer, G. M.; Ehlers, A. P.; Zumbusch, A.; Daltrozzo, E. *Angew. Chem., Int. Ed.* **2007**, *46*, 3750.

(8) (a) Sreejith, S.; Carol, P.; Chithra, P.; Ajayaghosh, A. *J. Mater. Chem.* **2008**, *18*, 264. (b) Mayerhöffer, U.; Fimmel, B.; Würthner, F. *Angew. Chem., Int. Ed.* **2012**, *51*, 164. (c) Ajayaghosh, A. *Acc. Chem. Res.* **2005**, *38*, 449.

(9) (a) Casado, J.; Ortiz, R. P.; Navarrete, J. T. L. *Chem. Soc. Rev.* **2012**, *41*, 5672.

(10) (a) Blake, I. M.; Anderson, H. L.; Beljonne, D.; Brédas, J.-L.; Clegg, W. *J. Am. Chem. Soc.* **1998**, *120*, 10764. (b) Zeng, W.; Lee, B. S.; Sung, Y. M.; Huang, K.-W.; Li, Y.; Kim, D.; Wu, J. *Chem. Commun.* **2012**, *48*, 7684. (c) Bill, N. L.; Ishida, M.; Bähring, S.; Lim, J. M.; Lee, S.; Davis, C. M.; Lynch, V. M.; Nielsen, K. A.; Jeppesen, J. O.; Ohkubo, K.; Fukuzumi, S.; Kim, D.; Sessler, J. L. *J. Am. Chem. Soc.* **2013**, *135*, 10852.

(11) (a) Sun, Z.; Zeng, Z.; Wu, J. *Acc. Chem. Res.* **2014**, *47*, 2582. (b) Chase, D. T.; Rose, B. D.; McClintock, S. P.; Zakharov, L. N.; Haley, M. M. *Angew. Chem., Int. Ed.* **2011**, *50*, 1127. (c) Chase, D. T.; Fix, A. G.; Rose, B. D.; Weber, C. D.; Nobusue, S.; Stockwell, C. E.; Zakharov, L. N.; Lonergan, M. C.; Haley, M. M. *Angew. Chem., Int. Ed.* **2011**, *50*, 11103. (d) Shimizu, A.; Kubo, T.; Uruichi, M.; Yakushi, K.; Nakano, M.; Shiomi, D.; Sato, K.; Takui, T.; Hirao, Y.; Matsumoto, K.; Kurata, H.; Morita, Y.; Nakasuji, K. *J. Am. Chem. Soc.* **2010**, *132*, 14421. (e) Shimizu, A.; Kishi, R.; Nakano, M.; Shiomi, D.; Sato, K.; Takui, T.; Hisaki, I.; Miyata, M.; Tobe, Y. *Angew. Chem., Int. Ed.* **2013**, *52*, 6076. (f) Nishida, J.-i.; Tsukaguchi, S.; Yamashita, Y. *Chem. - Eur. J.* **2012**, *18*, 8964.

(12) (a) Peierls, R. E. *Quantum Theory of Solids*; Oxford University Press: London, 1956. (b) Brédas, J. L. *J. Chem. Phys.* **1985**, *82*, 3808. (c) Risko, C.; McGehee, M. D.; Brédas, J. L. *Chem. Sci.* **2011**, *2*, 1200. (d) Kertesz, M.; Choi, C. H.; Yang, S. *Chem. Rev.* **2005**, *105*, 3448.

(13) Takahashi, T.; Matsuoka, K.-i.; Takimiya, K.; Otsubo, T.; Aso, Y. *J. Am. Chem. Soc.* **2005**, *127*, 8928.

(14) (a) Ortiz, R. P.; Casado, J.; Hernández, V.; Navarrete, J. T. L.; Viruela, P. M.; Ortí, E.; Takimiya, K.; Otsubo, T. *Angew. Chem., Int. Ed.* **2007**, *46*, 9057. (b) Ortiz, R. P.; Casado, J.; González, S. R.; Hernández, V.; Navarrete, J. T. L.; Viruela, P. M.; Ortí, E.; Takimiya, K.; Otsubo, T. *Chem.—Eur. J.* **2010**, *16*, 470. (c) Casado, J.; Navarrete, J. T. L. *Chem. Rec.* **2011**, *11*, 45. (d) Zotti, G.; Zecchin, S.; Vercelli, B.; Berlin, A.; Casado, J.; Hernández, V.; Ortiz, R. P.; Navarrete, J. T. L.; Ortí, E.; Viruela, P. M.; Milián, B. *Chem. Mater.* **2006**, *18*, 1539.

(15) (a) Zhang, C.; Zang, Y.; Gann, E.; McNeill, C. R.; Zhu, X.; Di, C.-a.; Zhu, D. *J. Am. Chem. Soc.* **2014**, *136*, 16176. (b) Pappenfus, T. M.; Chesterfield, R. J.; Frisbie, C. D.; Mann, K. R.; Casado, J.; Raff, J. D.; Miller, L. L. *J. Am. Chem. Soc.* **2002**, *124*, 4184. (c) Handa, S.; Miyazaki, E.; Takimiya, K.; Kunugi, Y. *J. Am. Chem. Soc.* **2007**, *129*, 11684. (d) Ribierre, J. C.; Fujihara, T.; Watanabe, S.; Matsumoto, M.; Muto, T.; Nakao, A.; Aoyama, T. *Adv. Mater.* **2010**, *22*, 1722. (e) Ribierre, J.-C.; Watanabe, S.; Matsumoto, M.; Muto, T.; Nakao, A.; Aoyama, T. *Adv. Mater.* **2010**, *22*, 4044. (f) Wu, Q.; Ren, S.; Wang, M.; Qiao, X.; Li, H.; Gao, X.; Yang, X.; Zhu, D. *Adv. Funct. Mater.* **2013**, *23*, 2277. (g) Qiao, Y.; Guo, Y.; Yu, C.; Zhang, F.; Xu, W.; Liu, Y.; Zhu, D. *J. Am. Chem. Soc.* **2012**, *134*, 4084. (h) Wu, Q.; Li, R.; Hong, W.; Li, H.; Gao, X.; Zhu, D. *Chem. Mater.* **2011**, *23*, 3138. (i) Handa, S.; Miyazaki, E.; Takimiya, K. *Chem. Commun.* **2009**, 3919. (j) Pappenfus, T. M.; Hermanson, B. J.; Helland, T. J.; Lee, G. G. W.; Drew, S. M.; Mann, K. R.; McGee, K. A.; Rasmussen, S. C. *Org. Lett.* **2008**, *10*, 1553. (k) Li, J.; Qiao, X.; Xiong, Y.; Li, H.; Zhu, D. *Chem. Mater.* **2014**, *26*, 5782.

(16) Ortiz, R. P.; Casado, J.; González, S. R.; Hernández, V.; Navarrete, J. T. L.; Viruela, P. M.; Ortí, E.; Takimiya, K.; Otsubo, T. *Chem.—Eur. J.* **2010**, *16*, 470.

(17) Casado, J.; Zgierski, M. Z.; Ewbank, P. C.; Burand, M. W.; Janzen, D. E.; Mann, K. R.; Rappenfus, T. M.; Berlin, A.; Pérez-Inestrosa, E.; Ortiz, R. P.; Navarrete, J. T. L. *J. Am. Chem. Soc.* **2006**, *128*, 10134.

(18) Zhu, X.; Tsuji, H.; Nakabayashi, K.; Ohkoshi, S.-i.; Nakamura, E. *J. Am. Chem. Soc.* **2011**, *133*, 16342.

(19) Yasuike, S.; Kurita, J.; Tsuchiya, T. *Heterocycles* **1997**, *45*, 1891.

(20) Suzuki, Y.; Miyazaki, E.; Takimiya, K. *J. Am. Chem. Soc.* **2010**, *132*, 10453.

(21) (a) Littke, A. F.; Dai, C.; Fu, G. C. *J. Am. Chem. Soc.* **2000**, *122*, 4020. (b) Yang, J.; Liu, S.; Zheng, J.-F.; Zhou, J. *Eur. J. Org. Chem.* **2012**, *2012*, 6248.

(22) Higuchi, H.; Yoshida, S.; Uraki, Y.; Ojima, J. *Bull. Chem. Soc. Jpn.* **1998**, *71*, 2229.

(23) (a) Jackson, N. E.; Savoie, B. M.; Kohlstedt, K. L.; de la Cruz, M. O.; Schatz, G. C.; Chen, L. X.; Ratner, M. A. *J. Am. Chem. Soc.* **2013**, *135*, 10475. (b) Pomerantz, M. *Tetrahedron Lett.* **2003**, *44*, 1563. (c) Turbiez, M.; Frère, P.; Allain, M.; Videlot, C.; Ackermann, J.; Roncali, J. *Chem. - Eur. J.* **2005**, *11*, 3742. (d) Guo, X.; Kim, F. S.; Jenekhe, S. A.; Watson, M. D. *J. Am. Chem. Soc.* **2009**, *131*, 7206. (e) Berrouard, P.; Grenier, F.; Pouliot, J.-R.; Gagnon, E.; Tessier, C.; Leclerc, M. *Org. Lett.* **2011**, *13*, 38. (f) Guo, X.; Ortiz, R. P.; Zheng, Y.; Kim, M.-G.; Zhang, S.; Hu, Y.; Lu, G.; Facchetti, A.; Marks, T. J. *J. Am. Chem. Soc.* **2011**, *133*, 13685. (g) Huang, H.; Chen, Z.; Ortiz, R. P.; Newman, C.; Usta, H.; Lou, S.; Youn, J.; Noh, Y.-Y.; Baeg, K.-J.; Chen, L. X.; Facchetti, A.; Marks, T. *J. Am. Chem. Soc.* **2012**, *134*, 10966. (h) Guo, X.; Zhou, N.; Lou, S. J.; Hennek, J. W.; Ortiz, R. P.; Butler, M. R.; Boudreault, P.-L. T.; Strzalka, J.; Morin, P.-O.; Leclerc, M.; Navarrete, J. T. L.; Ratner, M. A.; Chen, L. X.; Chang, R. P. H.; Facchetti, A.; Marks, T. J. *J. Am. Chem. Soc.* **2012**, *134*, 18427. (i) Guo, X.; Quinn, J.; Chen, Z.; Usta, H.; Zheng, Y.; Xia, Y.; Hennek, J. W.; Ortiz, R. P.; Marks, T. J.; Facchetti, A. *J. Am. Chem. Soc.* **2013**, *135*, 1986.

(24) (a) Mataga, N.; Yao, H.; Okada, T.; Rettig, W. *J. Phys. Chem.* **1989**, *93*, 3383. (b) Schütz, M.; Schmidt, R. *J. Phys. Chem.* **1996**, *100*, 2012.

(25) (a) Pan, Y.; Li, W.; Zhang, S.; Yao, L.; Gu, C.; Xu, H.; Yang, B.; Ma, Y. *Adv. Opt. Mater.* **2014**, *2*, 510. (b) Li, W.; Pan, Y.; Yao, L.; Liu,

DOI: 10.1021/jacs.5b03899
J. Am. Chem. Soc. 2015, 137, 11294−11302

H.; Zhang, S.; Wang, C.; Shen, F.; Lu, P.; Yang, B.; Ma, Y. *Adv. Opt. Mater.* **2014**, *2*, 892. (c) Li, W.; Pan, Y.; Xiao, R.; Peng, Q.; Zhang, S.; Ma, D.; Li, F.; Shen, F.; Wang, Y.; Yang, B.; Ma, Y. *Adv. Funct. Mater.* **2014**, *24*, 1609. (d) Zhang, S.; Li, W.; Yao, L.; Pan, Y.; Shen, F.; Xiao, R.; Yang, B.; Ma, Y. *Chem. Commun.* **2013**, *49*, 11302. (e) Li, W.; Liu, D.; Shen, F.; Ma, D.; Wang, Z.; Feng, T.; Xu, Y.; Yang, B.; Ma, Y. *Adv. Funct. Mater.* **2012**, *22*, 2797. (f) Tang, S.; Li, W.; Shen, F.; Liu, D.; Yang, B.; Ma, Y. *J. Mater. Chem.* **2012**, *22*, 4401.

(26) (a) Adachi, C.; Baldo, M. A.; Forrest, S. R.; Thompson, M. E. *J. Appl. Phys.* **1999**, *11*, 285. (b) Greenham, N. C.; Friend, R. H.; Bradley, D. D. C. *Adv. Mater.* **1994**, *6*, 491.

(27) (a) Uoyama, H.; Goushi, K.; Shizu, K.; Nomura, H.; Adachi, C. *Nature* **2012**, *492*, 234. (b) Tao, Y.; Yuan, K.; Chen, T.; Xu, P.; Li, H.; Chen, R.; Zhang, C.; Zhang, L.; Huang, W. *Adv. Mater.* **2014**, *26*, 7931. (c) Goushi, K.; Yoshida, K.; Sato, K.; Adachi, C. *Nat. Photonics* **2012**, *6*, 253. (d) Zhang, Q.; Li, B.; Huang, S.; Nomura, H.; Tanaka, H.; Adachi, C. *Nat. Photonics* **2014**, *8*, 326.

(28) Patra, A.; Wijsboom, Y. H.; Leitus, G.; Bendikov, M. *Chem. Mater.* **2011**, *23*, 896.

DOI: 10.1021/jacs.5b03899
J. Am. Chem. Soc. 2015, 137, 11294−11302